ACS APPLIED MATERIALS & INTERFACES

Research Article

www.acsami.org

Engineered Biochar from Biofuel Residue: Characterization and Its Silver Removal Potential

Ying Yao,[†,‡,§] Bin Gao,[*,§] Feng Wu,[*,†,‡] Cunzhong Zhang,[†,‡] and Liuyan Yang[∥]

[†]Beijing Key Laboratory of Environmental Science and Engineering, School of Chemical Engineering and the Environment, Beijing Institute of Technology, Beijing 100081, China

[‡]National Development Center of High Technology Green Materials, Beijing 100081, China

[§]Department of Agricultural and Biological Engineering, University of Florida, Gainesville, Florida 32611, United States

[∥]School of the Environment, Nanjing University, Nanjing 210046, China

ABSTRACT: A novel approach was used to prepare engineered biochar from biofuel residue (stillage from bagasse ethanol production) through slow pyrolysis. The obtained biochar was characterized for its physicochemical properties as well as silver sorption ability. Sorption experimental data showed that engineered biochar quickly and efficiently removed silver ion (Ag^+) from aqueous solutions with a Langmuir maximum capacity of 90.06 mg/g. The high sorption of Ag^+ onto the biochar was attributed to both reduction and surface adsorption mechanisms. The reduction of Ag^+ by the biochar was confirmed with scanning electron microscopy, energy-dispersive X-ray spectroscopy, X-ray diffraction, and X-ray photoelectron spectroscopy analyses of the postsorption biochar, which clearly showed the presence of metallic silver nanoparticles on the surface of the carbon matrix. An antimicrobial ability test indicated that silver-laden biochar effectively inhibited the growth of *Escherichia coli*, while the original biochar without silver nanoparticles promoted growth. Thus, biochar, prepared from biofuel residue materials, could be potentially applied not only to remove Ag^+ from aqueous solutions but also to produce a new value-added nanocomposite with antibacterial ability.

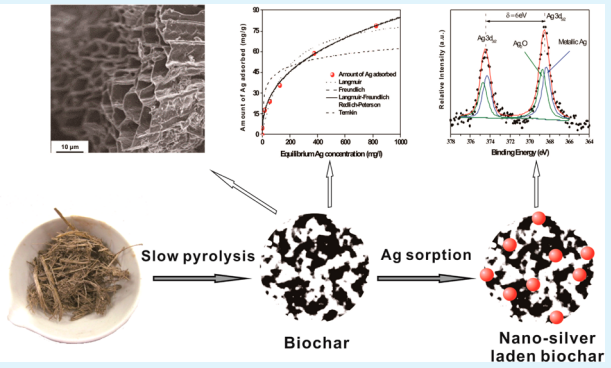

KEYWORDS: *biochar, engineered carbon, biofuel residue, silver, nanocomposite*

INTRODUCTION

Engineered carbon/biochar, which has been attracting tremendous research interest recently, is pyrogenic carbon converted from various biomass materials like agricultural, forestry, and other waste residues through thermal pyrolysis in an oxygen-limited environment. It has great potential to be used in soil amendment and/or as a low-cost sorbent to sequester carbon, enhance soil fertility, and benefit the environment, as widely highlighted in recent studies.[1−3] As a consequence, the conversion of biomass into biochar, considered as one of the most popular bioenergy conversion technologies, has received significant attention from both government regulation agencies and the general public.[4]

Stillage (sludge) from bagasse ethanol production is the residual material derived from a bioethanol production process after distillation. Utilization of stillage as a fuel or source of biofuel and biochar production could improve energy efficiency as well as add value to the stillage. Several studies have been conducted to explore the potential of biofuel production such as methane from the bagasse, but limited attention has been paid to biochar conversion through thermal pyrolysis from ethanol stillage bagasse or possible uses of its residues.[5]

Currently, commercial bioethanol production processes tend to utilize nonfood biomass resources such as agricultural residues and urban wastes instead of classic crops like sugar cane and wheat, aiming to fight the world food supply scarcity today.[6] In these feedstocks, the predominant carbohydrates converted to ethanol are the polymer cellulose and hemicellulose. In a typical process, cellulosic materials are first subjected to biological and/or thermochemical pretreatment in order to hydrolyze cellulose and hemicellulose to sugars. A recombinant *Eschericha coli* is employed to ferment both the hexose and pentose sugars to ethanol after a dilute acid hydrolysis and an enzymatic hydrolysis. Ethanol is finally produced and collected during distillation, which generates a byproduct called stillage.[7] Stillage is generally considered to be a high-volume, high-strength waste that presents significant disposal or treatment problems.[5]

Alternatively, stillage residue has great potential as feedstock material for biochar production application, which could improve the energy efficiency and reduce the carbon footprint

Received: April 10, 2015
Accepted: April 29, 2015
Published: April 29, 2015

DOI: 10.1021/acsami.5b03131
ACS Appl. Mater. Interfaces 2015, 7, 10634−10640

Table 1. Elemental Analysis of Biochars Produced in This Study (Mass %)[a]

	% mass based[b]													
biochar	P	K	Na	Mg	Ca	Cu	Cr	Fe	Al	As	Cd	Ag	Mn	Pb
EBG	0.28	0.03	0.08	0.07	0.12	0.01	-	0.10	0.02	-	-	-	-	-
BG[c]	0.08	0.15		0.21	0.91	0.00	-	0.05	0.11	-	-	-	0.00	0.00

[a]EBG and BG are biochars produced from ethanol stillage and raw bagasse, respectively. [b]- below the detection limit. [c]Data from our previous work.[39]

of the bioethanol production process. Ethanol stillage residue bagasse used in this work is a carbon-rich biomass, primarily consisting of 23% cellulose, 4.3% hemicellulose, 20% lignin, and 14.06% protein,[5] which makes it suitable for biochar production. Thus, this bioenergy conversion of stillage residue could be a viable, ecofriendly, and sustainable approach that may bring about multiple environmental and economic benefits.

In this study, we investigated the conversion of bioethanol stillage residue obtained from the Biofuel Pilot Plant at the University of Florida to biochar through slow pyrolysis. The physicochemical properties of the engineered biochar were characterized, and its potential environmental applications were evaluated by measuring the sorption characteristics to silver ions (Ag^+). Ag^+ have been classified as hazardous substances in water systems by the World Health Organization and the U.S. Environmental Protection Agency because of its extensive application in dentistry, clothing, the food industry, and jewelry manufacturing.[8−11] The specific objectives of this work were as follows: (1) development of a novel approach to managing bioenergy residues, (2) characterization of the obtained biochar's physicochemical properties, (3) assessment of their ability to remove Ag^+ from aqueous solutions, and (4) determination of the governing mechanisms of silver sorption on the biochar.

EXPERIMENTAL SECTION

Materials. Stillage residue collected from the Biofuel Pilot Plant at University of Florida was used as raw materials for biochar production. The pilot plant produces ethanol from sugar cane bagasse using a dilute acid−steam process (1% phosphoric acid) to solubilize lignocellulosic biomass into a form for which enzymatic hydrolysis is effective. A recombinant *E. coli* KO11 strain, developed in the Microbiology and Cell Science Department, is employed to ferment both hexose and pentose sugars to ethanol.[12] The stillage residue was collected and dried after the distillation process, in which ethanol was separated from the fermentation broth at 60 °C.

The stillage residue was dried in an oven at 60 °C and ground into 1−2 mm pieces as a feedstock for biochar production. A tube furnace (MTI, Richmond, CA) was used to pyrolyze them into biochar in a N_2 environment at a temperature of 600 °C for 1 h. The resulting biochar (labeled as EBG) was washed several times with deionized water and dried at 60 °C for further tests. Detailed information about biochar production procedures can be found in previous studies.[13]

Sorption Experiments. The characteristics and mechanisms of silver sorption onto EBG were studied using sorption kinetic and isotherm experiments. For each experiment, 0.05 g of the sorbent was mixed with 25 mL of a silver solution in the digestion vessel. The mixture was then shaken at 55 rpm on a horizontal shaker at room temperature. To measure the sorption kinetics, 100 mg/L silver solutions were used in a range of contact time intervals (10 and 30 min and 1, 2, 6, 12, and 24 h). To obtain sorption isotherms, different concentrations of a silver solution (i.e., 0, 10, 50, 100, 200, 500, and 1000 mg/L) were mixed with 0.05 g of the EBG biochar sorbent and shaken for 24 h (sufficient to reach adsorption equilibrium). At the end of each experiment, the mixtures were immediately filtered through 0.22-μm-pore-size nylon membranes (GE cellulose nylon membranes). The silver contents on the solid phase were calculated based on the initial and final aqueous concentrations, which were determined by inductively coupled plasma atomic emission spectroscopy (ICP-AES). The postadsorption biochar samples were collected, rinsed with deionized water, and dried at 80 °C for further experiments.

Characterizations. A range of physicochemical properties of the original and silver-sorbed ethanol residue bagasse biochar (EBG) were investigated in detail. Major elements of biochar were determined by acid digestion of the samples followed by ICP-AES analysis. Scanning electron microscopy (SEM) imaging analyses were conducted using a JEOL JSM-6400 scanning electron microscope to obtain the structure and surface characteristics of the samples. Surface elemental analysis was also conducted simultaneously at the same spot using energy-dispersive X-ray spectroscopy (EDX; Oxford Instruments Link ISIS) along with SEM. EDX analysis can provide rapid qualitative, or with adequate standards, semiquantitative analysis of elemental composition with a depth of 1−2 μm.[14] X-ray diffraction (XRD) analyses were conducted to identify crystalline structures on the silver-loaded sorbents using a computer-controlled X-ray diffractometer (Philips Electronic Instruments) with nickel-filtered Cu Ka radiation (λ = 1.5406 Å), which is equipped with a stepping motor and a graphite crystal monochromator. Crystalline compounds in the samples were identified by comparing diffraction data against a database compiled by the Joint Committee on Powder Diffraction and Standards. X-ray photoelectron spectroscopy (XPS) measurements were carried out on a PHI Quantera II system (Ulvac-PHI Inc., Japan) to determine the oxidation states of the silver species sorbed on the sample surface.

Antimicrobial Ability. In order to obtain silver-laden biochar for conducting microbial growth inhibition experiments, 0.2 g of EBG was mixed with 100 mL of a silver solution (1000 mg/L) and shaken for 24 h. After filtration, silver-laden biochar samples were collected and dried at 80 °C (referred to as EBG-Ag). The amount of adsorbed silver in the EBG-Ag samples was around 79.02 mg/g.

Microbial growth inhibition tests of EBG and EBG-Ag were conducted with *E. coli* DH5α. The bacteria were cultured overnight at 37 °C by constant agitation in a biochemical incubator (Senxin GRP-9160, Shanghai, China). About 50 mg of sterile (autoclaved at 121 °C for 15 min) EBG or EBG-Ag was added to 5 mL of a fresh nutrient broth medium [each group contained 10^5 cfu/mL (cfu = colony-forming units) of *E. coli*] to test their effects on bacterial growth. Previous studies have shown that the sterile process has no effect on the biochar and silver during autoclaving.[15,16] The mixtures were incubated at 37 °C for 18 h. Blank controls with no biochar sample addition were also tested. The pour-plate method was used to enumerate *E. coli* following APHA standard procedures.[17] Briefly, about 0.2 mL of the diluted *E. coli*−sorbent mixtures was placed in the center of a sterile Petri dish (100 mm diameter) using a sterile pipet. Sterile molten agar (45−50 °C) was added to each plate and then mixed gently by swirling. The mixtures were allowed to cool until solidified and then were incubated at 37 °C for 18 h. Colonies in the medium were counted to determine bacterial abundance following APHA standard procedures. The growth experiments were repeated nine times for each treatment, and the results were statistically analyzed using the Student t test and one-way ANOVA with a significance level of 0.05 ($p < 0.05$).

DOI: 10.1021/acsami.5b03131
ACS Appl. Mater. Interfaces 2015, 7, 10634−10640

RESULTS AND DISCUSSION

EBG was produced through slow pyrolysis with a production rate of 26.7% on a weight basis, which is comparable with that of other biochars from different feedstock types and also very close to that of raw bagasse biochar reported in previous studies.[18] After agricultural residues were first fermented and distilled to produce biofuel, the bioenergy in biofuel stillage could be further converted into biochar by this biochar production approach, which could have potential application in the fields of both environment and electrochemistry. Thus, we could make full use of agricultural residues and achieve the greatest economic benefits.

Elemental analysis of EBG biochar indicated that all of the element contents of EBG were comparable to biochar made from raw bagasse feedstock, while the contents of the elements potassium, magnesium, and calcium were slightly lower than that of raw bagasse biochar (BG; Table 1), probably because of bacterial consumption of these nutrient elements during fermentation in ethanol production processes. Elemental analysis results further confirmed that biochar was successfully produced from ethanol stillage residue feedstock.

Silver Sorption by EBG Biochar. Initial evaluation showed that EBG biochar could effectively remove Ag^+ from aqueous solution with a removal rate of 97.4% when the original Ag^+ concentration was 20.7 mg/L. In order to better understand the processes governing the adsorption of silver to the engineered biochar and its sorption capacity, kinetic and isotherm studies were carried out and a number of well-known sorption models were applied.

The kinetic experimental data shows a rapid initial uptake followed by a smooth increase, with equilibrium reached in less than 24 h (Figure 1). Different mathematical models including

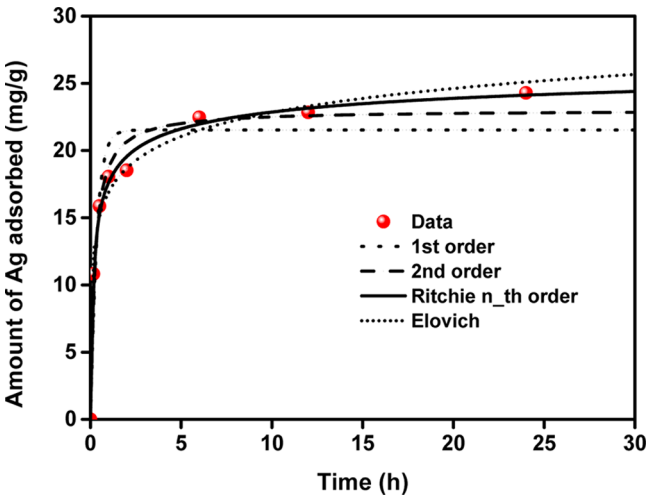

Figure 1. Adsorption kinetic data and modeling for silver on EBG. Symbols are experimental data, and lines are model results.

the pseudo-first-order, pseudo-second-order, Ritchie *n*th-order, and Elovich models were used to fit the kinetic data, and the governing equations are listed as

$$\frac{dq_t}{dt} = k_1(q_e - q_t), \quad \text{first-order} \tag{1.1}$$

$$\frac{dq_t}{dt} = k_2(q_e - q_t)^2, \quad \text{second-order} \tag{1.2}$$

$$\frac{dq_t}{dt} = k_n(q_e - q_t)^n, \quad \text{Ritchie } n\text{th-order} \tag{1.3}$$

$$\frac{dq_t}{dt} = \alpha \exp(-\beta q_t), \quad \text{Elovich} \tag{1.4}$$

where q_t (mg/g) and q_e (mg/g) are the amount of silver adsorbed at time t and the equilibrium state, respectively, k_1 (h^{-1}), k_2 (g/mg·h), and k_n (g^{n-1}/mg^{n-1}·h) are adsorption rate constants for the first-order, second-order, and Ritchie *n*th-order models, respectively, α (mg/g·h) is the initial adsorption rate, and β (g/mg) is the desorption constant. More details can be found in our previous studies.[19] The best-fit kinetic model parameters are listed in Table 2. All of these models reproduced the kinetic data pretty well (Figure 1) with coefficients of determination (R^2) exceeding 0.93. Among the four kinetic models tested, the Ritchie *n*th-order model fits the experimental data better with R^2 of 0.997, revealing that silver sorption to the engineered biochar could be controlled by multiple mechanisms.

The adsorption equilibrium isotherm is important for describing how the adsorbate molecules distribute between the liquid and solid phases under the equilibrium state.[20] The isotherm experiment results shown in Figure 2 indicate that ethanol stillage biochar has a great silver adsorption ability of over 90 mg/L. Four well-known models were used to fit the isotherm experimental data that is essential to practical operation, and the governing equations are[21,22]

$$q_e = \frac{KQC_e}{1 + KC_e}, \quad \text{Langmuir} \tag{2.1}$$

$$q_e = K_f C_e^{\,n}, \quad \text{Freundlich} \tag{2.2}$$

$$q_e = \frac{K_{lf} Q C_e^{\,n}}{1 + K_{lf} C_e^{\,n}}, \quad \text{Langmuir–Freundlich} \tag{2.3}$$

$$q_e = \frac{K_r C_e}{1 + a C_e^{\,n}}, \quad \text{Redlich–Peterson} \tag{2.4}$$

$$q_e = \frac{RT}{b} \ln(AC_e), \quad \text{Temkin} \tag{2.5}$$

where K (L/mg), K_f (mg^{1-n}·L^n/g), K_{lf} (L^n/mg^n), and K_r (L/g) represent the four models' coefficients, respectively, Q (mg/g) denotes the maximum capacity, C_e (mg/L) is the sorbate concentration at equilibrium, and n (dimensionless), a (L^n/mg^n), and b (J·g/mg) and A (L/mg) are constants for the Freundlich, Redlich–Peterson, and Temkin isotherm models, respectively.[22] See the details in work by Yao et al.[19] Except Temkin, all of the other four tested isotherm models fit the experimental data fairly well with R^2 over 0.963, and the parameters are also shown in Table 2. The Langmuir maximum capacity of EBG was around 90.06 mg/g, which was much higher than that of many other adsorbents for silver sorption from aqueous solutions.[23,24] For example, Praus et al.[25] reported that montmorillonite only showed a silver sorption capacity of 42.1 mg/g. In addition, the Freundlich, Langmuir–Freundlich, and Redlich-Peterson models had better fitting than the other two, with R^2 values of 0.997, 0.996, and 0.997, respectively. The above results revealed that silver sorption onto EBG was likely controlled by heterogeneous processes with multilayer sorption, and the process could be governed by

DOI: 10.1021/acsami.5b03131
ACS Appl. Mater. Interfaces 2015, 7, 10634–10640

Table 2. Best-Fit Kinetic and Isotherm Model Parameters for Silver Adsorption to the Engineered Biochar

	parameter 1	parameter 2	parameter 3	R^2
		Adsorption Kinetics		
first-order	k_1 = 3.024 h^{-1}	q_e = 21.53 mg/g		0.931
second-order	k_2 = 0.191 g/mg·h	q_e = 23.02 mg/g		0.981
*n*th-order	k_n = 7.834 g^{n-1}/mg^{n-1}·h	q_e = 28.50 mg/g	n = 4.458	0.996
Elovich	β = 2.578 g/mg	α = 272.72 mg/g·h		0.956
		Adsorption Isotherms		
Langmuir	K = 0.006 L/mg	Q = 90.06 mg/g		0.963
Freundlich	K_f = 5.513 mg^{1-n}·L^n/g	n = 0.397		0.997
Langmuir–Freundlich	K_{lf} = 0.008 L^n/mg^n	Q = 600.20 mg/g	n = 0.449	0.996
Redlich–Peterson	K_r = 17.99 L/g	a = 100.00 L^n/mg^n	n = 0.604	0.997
Temkin	b = 309.10 J·g/mg	A = 2.465 L/mg		0.766

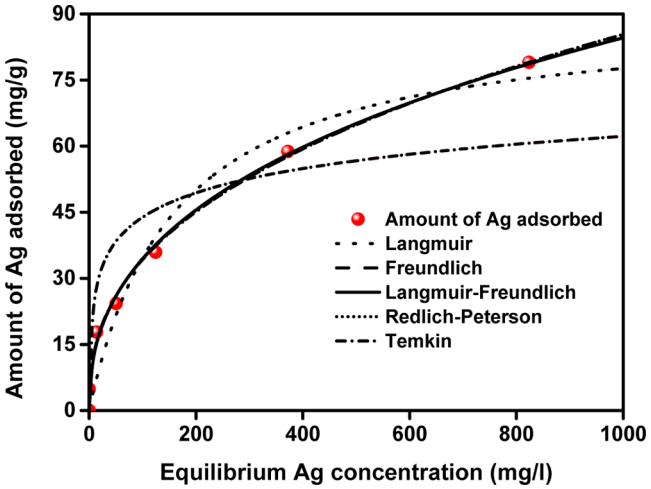

Figure 2. Adsorption isotherm data and modeling for silver on EBG. Symbols are experimental data, and lines are model results.

multiple mechanisms, which is consistent with kinetic study results.[22]

SEM–EDX, XRD, and XPS. In order to investigate the morphological structure, the engineered biochar samples were observed by SEM. In general, the morphology of the original biochar (EBG) was porous with a rough surface probably because of the intrinsic nature of the bagasse feedstock (Figure 3A). SEM observation, as shown in Figure 3B, also demonstrated that the obtained biochar consists of microsized carbon tubes.

After silver adsorption, the SEM image of the biochar showed that a significant amount of silver particles were attached to the biochar surface (Figure 3C,D), which were not found on the original biochar sample. Silver nanoparticles were deposited on the surface of the porous carbon matrix, which included not only the biochar particle surface but also the inner pore surfaces. The EDX spectrum (Figure 4) of the surface at the same spot as SEM imaging identified these nanoparticles as mainly silver species because of extremely high peaks of silver observed, which suggests that silver from aqueous solution was successfully adsorbed onto the carbon surface and/or into the matrix.

XRD analysis of the postsorption biochar revealed the presence of silver crystals that was not detected on the original char (Figure 5). In the XRD pattern, four strong diffraction peaks at 38.2°, 44.2°, 64.3°, and 77.1° on silver-sorbed biochar could be indexed to metallic silver facets of (111), (200), (220), and (311), respectively.[9,26] The XRD result concurs with the SEM–EDX analyses that the surface of the biochar after silver adsorption was widely covered by silver particles.

The particle size of silver nanorods within the biochar matrix was estimated using the Scherrer equation (3.1), which was designed in 1918 for determination of the mean size of single-crystal nanoparticles or crystallites in nanocrystalline bulk materials:[27,28]

$$\tau = \frac{K\lambda}{\beta \cos\theta} \tag{3.1}$$

where K is the shape factor with a typical value of about 0.9, λ is the X-ray wavelength, β is the line broadening at half of the maximum intensity (fwhm) in radians, and θ is the Bragg angle; τ is the mean size of the ordered (crystalline) domains. The average grain size of silver crystals within the biochar matrix in this study was about 27.8 ± 2.4 nm based on the calculation results of the four peaks selected. The XRD results concurred with SEM–EDX analyses and demonstrated that the engineered biochar produced from ethanol sludge residue has the ability to strongly adsorb silver from aqueous solution and could also form silver nanoparticles on the carbon matrix surfaces including inner pore surfaces as long as Ag^+ in the aqueous solution could diffuse through the biochar matrix and penetrate into the inner pores. These newly formed nanocomposites based on the silver-sorbed biochar could have potential usage in energy storage devices, such as lithium–air battery because silver on a carbon substrate showed great performance in the lithium–air cell.

The adsorption of silver on the biochar was further confirmed by XPS analysis (Figure 6). The spectrum of Ag 3d shows that the $3d_{3/2}$ and $3d_{5/2}$ signals are located at 374.50 and 368.50 eV, respectively. The splitting of the 3d doublet is 6.0 eV. The Ag $3d_{3/2}$ and $3d_{5/2}$ spectra clearly show the presence of two silver species, i.e., metallic (zerovalent) silver and silver oxide (Ag_2O), on the postsorption biochar surface (Figure 6). Because metallic silver will be oxidized spontaneously upon exposure to O_2 (ΔG_{rxn}° = −22.6 kJ < 0),[29] Ag_2O in the EBG-Ag sample was formed probably because of oxidization of metallic silver on the carbon surface by air, which is commonly referred to as "tarnishing".

Adsorption Mechanisms. The intense sorption of Ag^+ by EBG biochar was mainly attributed to both reduction and surface adsorption mechanisms. The XRD spectrum shows the presence of metallic silver nanoparticles on the surface of a biochar matrix after adsorption processes, which indicated that Ag^+ in the solution was reduced and precipitated on the carbon surface. Previous studies demonstrated that biochar could act as both electron donor/acceptor and participate in redox

DOI: 10.1021/acsami.5b03131
ACS Appl. Mater. Interfaces 2015, 7, 10634–10640

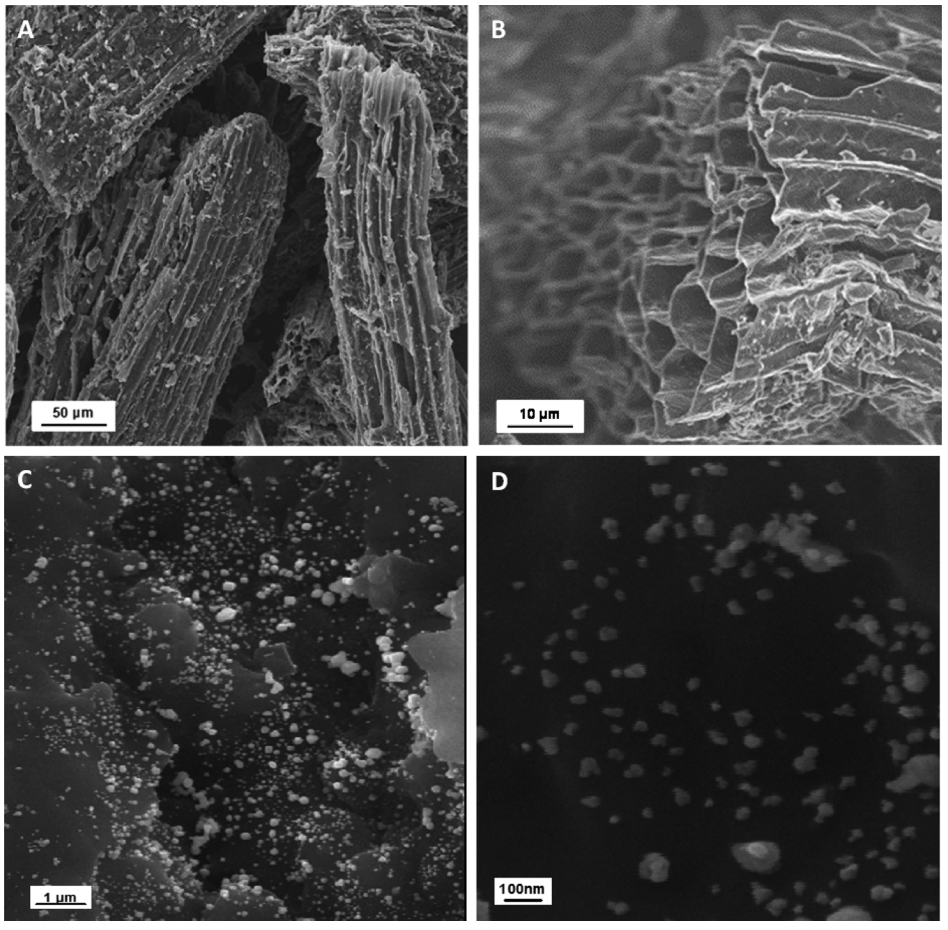

Figure 3. SEM images of the (A and B) original and (C and D) EBG-Ag morphological structures.

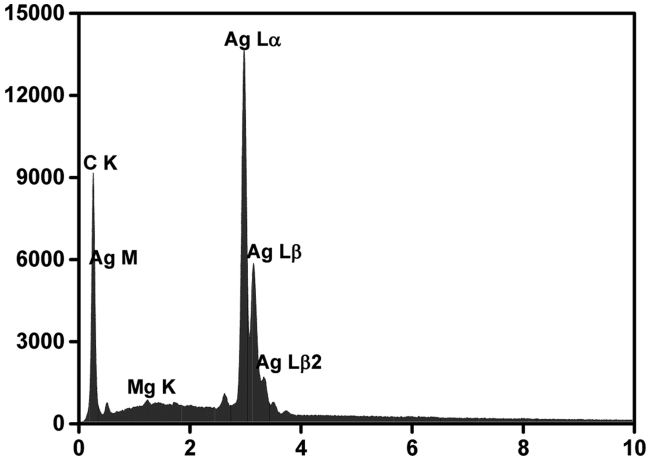

Figure 4. EDX spectrum of EBG-Ag morphological structures.

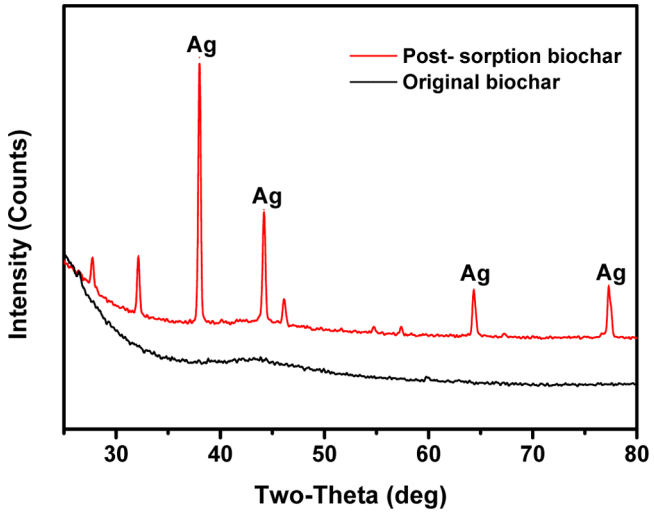

Figure 5. XRD spectra of the original and EBG-Ag.

reactions, which can be ascribed to aromatic, quinone structures, and functional groups (carboxyl, hydroxyl, and amino groups) in the carbon matrix.[30−33] Klüpfel et al. reported that biochars from plant biomass can take up and release several hundred micromoles of electrons per gram of biochar.[33] Dong et al. showed evidence that carboxyl groups in biochar derived from sugar beet tailings were capable of reducing Cr^{VI} to Cr^{III}.[32] Equations 4.1−4.3 give examples of hydroxyl, carbonyl, and carboxyl groups donating electrons:

$$BS{-}CH_2OH + 2Ag^+ + 2OH^- \rightarrow BS{-}CHO + 2Ag^0 + 2H_2O \quad (4.1)$$

$$BS{-}CHO + 2Ag^+ + 2OH^- \rightarrow BS{-}COOH + 2Ag^0 + H_2O \quad (4.2)$$

$$BS{-}COOH + Ag^+ \rightarrow BS + CO_2 \uparrow + Ag^0 + H^+ \quad (4.3)$$

DOI: 10.1021/acsami.5b03131
ACS Appl. Mater. Interfaces 2015, 7, 10634−10640

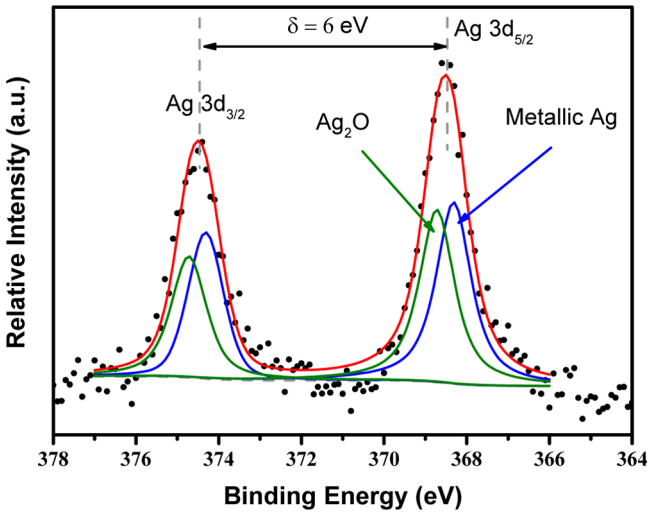

Figure 6. XPS spectra of the Ag $3d_{3/2}$ and $3d_{5/2}$ regions for EBG-Ag.

where BS represents the biochar surface. After reduction, the newly formed metallic silver prefers to nucleate and grow on the carbon surface within the biochar because of lower surface energy,[19,34] which was confirmed by examination of the morphology and crystallization of the particles shown in the SEM, EDX, and XRD results.

In addition, biochar surfaces are known to have a net negative charge similar to sand and soil;[35,36] the number of negatively charged sites on EBG biochar could likely bind Ag^+, as is evident by XPS analysis, which could be another possible mechanism for silver sorption.

Antimicrobial Ability. Because silver nanoparticles have long been known to possess dramatic antimicrobial ability, EBG-Ag biochar has a potential application as a value-added antibacterial/antifungal agent. An *E. coli* growth inhibition test was thus carried out, and the growth response showed dramatic differences among EBG, EBG-Ag, and blank control groups (Figure 7). The growth of bacterial colonies in EBG and blank control samples reached the order of 10^7 cfu/mL, while that in EBG-Ag samples was only on the order of 10^5 cfu/mL. The bacteria concentrations of EBG and control groups were 2 orders of magnitude higher than that of the EBG-Ag sample. In order to statistically analyze the differences between the three group means and their associated procedures, the one-way ANOVA (analysis of variance), a collection of statistical models, was carried out. The results showed statistically significant differences in the bacterial growth number among these three treatments ($p = 1.41 \times 10^{-27}$), suggesting that the silver-laden biochar does have an obvious antibiotic effect on *E. coli* and could act as a potential antimicrobial agent. The average number of bacteria in EBG media was 6.7×10^7 cfu/mL, which was statistically higher than that in blank control media (5.3×10^7 cfu/mL) with $p < 0.001$, implying that silver-free biochar could actually promote bacterial growth. This is in line with the findings of previous studies that biochar soil amendment often benefits soil microorganisms by providing suitable habitats, additional organic carbon, and mineral nutrient sources.[37]

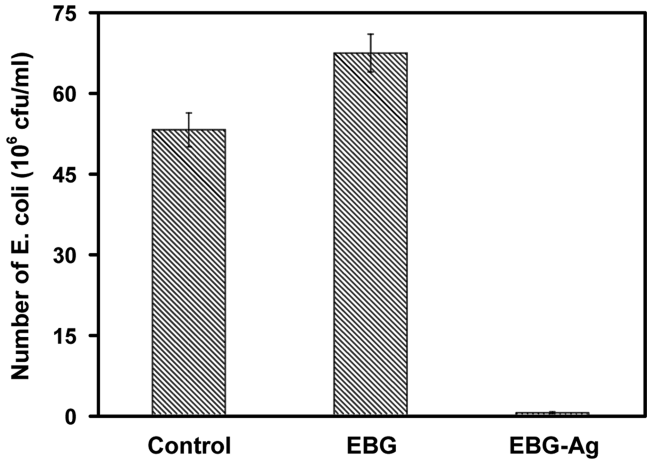

Figure 7. Effects of EBG and EBG-Ag on the growth of *E. coli*.

CONCLUSION

This study developed a novel approach to directly converting bioenergy from biofuel residue to biochar and demonstrated that this bioenergy conversion method of stillage residue is viable, ecofriendly, and sustainable, which could benefit the environment as well as the economic profits. The obtained biochar (EBG) not only effectively sorbed Ag^+ from aqueous solutions but also reclaimed the silver to form a value-added nanocomposite (EBG-Ag) with stabilized silver nanoparticles on biochar surfaces. The sorption ability of EBG was mainly attributed to the mechanism of reduction by the carbon matrix and surface adsorption. The postsorption biochar containing a large quantity of silver nanoparticles showed strong antimicrobial ability and thus could be used as an antibacterial/antifungal agent in various applications, particularly environmental applications. In addition, given the catalytic activity that silver nanostructures showed in the lithium−air battery,[38] the silver nanocomposite in the carbon matrix could potentially open a new window for the application of biochar in energy storage devices, especially in the lithium−air battery.

AUTHOR INFORMATION

Corresponding Authors

*E-mail: bg55@ufl.edu. Tel: 1-(352)-392-1864 ext. 285.
*E-mail: wufeng863@bit.edu.cn. Tel: 86-10-68912508.

Notes

The authors declare no competing financial interest.

ACKNOWLEDGMENTS

This research was partially supported by the National Natural Science Foundation of China through Grant 51402018 and the National Science Foundation through Grant CBET-1054405. The authors also thank Dr. Lonnie Ingram for providing the biofuel residue.

REFERENCES

(1) Marris, E. Putting the Carbon Back: Black Is the New Green. *Nature* **2006**, *442* (7103), 624−626.
(2) Lehmann, J. A Handful of Carbon. *Nature* **2007**, *447* (7141), 143−144.
(3) Woolf, D.; Amonette, J. E.; Street-Perrott, F. A.; Lehmann, J.; Joseph, S. Sustainable Biochar to Mitigate Global Climate Change. *Nat. Commun.* **2010**, *1*, 56.
(4) Inyang, M.; Gao, B.; Pullammanappallil, P.; Ding, W.; Zimmerman, A. R. Biochar from Anaerobically Digested Sugarcane Bagasse. *Bioresour. Technol.* **2010**, *101* (22), 8868−72.

DOI: 10.1021/acsami.5b03131
ACS Appl. Mater. Interfaces 2015, 7, 10634−10640

(5) Tian, Z.; Mohan, G. R.; Ingram, L.; Pullammanappallil, P. Anaerobic Digestion for Treatment of Stillage from Cellulosic Bioethanol Production. *Bioresour. Technol.* **2013**, *144*, 387−95.
(6) Demirbas, A. Competitive Liquid Biofuels from Biomass. *Appl. Energy* **2011**, *88* (1), 17−28.
(7) Wilkie, A. C.; Riedesel, K. J.; Owens, J. M. Stillage Characterization and Anaerobic Treatment of Ethanol Stillage from Conventional and Cellulosic Feedstocks. *Biomass Bioenergy* **2000**, *19* (2), 63−102.
(8) *Secondary Drinking Water Regulations: Guidance for Nuisance Chemicals*; U.S. Environmental Protection Agency: Washington, DC, 2013.
(9) Zhou, Y.; Gao, B.; Zimmerman, A. R.; Cao, X. Biochar-Supported Zerovalent Iron Reclaims Silver from Aqueous Solution to Form Antimicrobial Nanocomposite. *Chemosphere* **2014**, *117*, 801−805.
(10) Eckelman, M. J.; Graedel, T. Silver Emissions and Their Environmental Impacts: A Multilevel Assessment. *Environ. Sci. Technol.* **2007**, *41* (17), 6283−6289.
(11) Johnson, J.; Jirikowic, J.; Bertram, M.; Van Beers, D.; Gordon, R.; Henderson, K.; Klee, R.; Lanzano, T.; Lifset, R.; Oetjen, L. Contemporary Anthropogenic Silver Cycle: A Multilevel Analysis. *Environ. Sci. Technol.* **2005**, *39* (12), 4655−4665.
(12) Geddes, C. C.; Nieves, I. U.; Ingram, L. O. Advances in Ethanol Production. *Curr. Opin. Biotechnol.* **2011**, *22* (3), 312−319.
(13) Yao, Y.; Gao, B.; Chen, J.; Zhang, M.; Inyang, M.; Li, Y.; Alva, A.; Yang, L. Engineered Carbon (Biochar) Prepared by Direct Pyrolysis of Mg-Accumulated Tomato Tissues: Characterization and Phosphate Removal Potential. *Bioresour. Technol.* **2013**, *138*, 8−13.
(14) Martins, R.; Bahia, M.; Buono, V. Surface Analysis of Profile Instruments by Scanning Electron Microscopy and X-Ray Energy-Dispersive Spectroscopy: A Preliminary Study. *Int. Endod. J.* **2002**, *35* (10), 848−853.
(15) Venkatesham, M.; Ayodhya, D.; Madhusudhan, A.; Babu, N. V.; Veerabhadram, G. A Novel Green One-Step Synthesis of Silver Nanoparticles Using Chitosan: Catalytic Activity and Antimicrobial Studies. *Appl. Nanosci.* **2014**, *4* (1), 113−119.
(16) Yao, Y.; Gao, B.; Chen, H.; Jiang, L.; Inyang, M.; Zimmerman, A. R.; Cao, X.; Yang, L.; Xue, Y.; Li, H. Adsorption of Sulfamethoxazole on Biochar and Its Impact on Reclaimed Water Irrigation. *J. Hazard. Mater.* **2012**, *209−210*, 408−13.
(17) *Standard Methods for the Examination of Water and Wastewater*, 19th ed.; American Public Health Association: Washington, DC, 1995.
(18) Sun, Y.; Gao, B.; Yao, Y.; Fang, J.; Zhang, M.; Zhou, Y.; Chen, H.; Yang, L. Effects of Feedstock Type, Production Method, and Pyrolysis Temperature on Biochar and Hydrochar Properties. *Chem. Eng. J.* **2014**, *240*, 574−578.
(19) Yao, Y.; Gao, B.; Chen, J.; Yang, L. Engineered Biochar Reclaiming Phosphate from Aqueous Solutions: Mechanisms and Potential Application as a Slow-Release Fertilizer. *Environ. Sci. Technol.* **2013**, *47* (15), 8700−8.
(20) Almeida, C.; Debacher, N.; Downs, A.; Cottet, L.; Mello, C. Removal of Methylene Blue from Colored Effluents by Adsorption on Montmorillonite Clay. *J. Colloid Interface Sci.* **2009**, *332* (1), 46−53.
(21) Yao, Y.; Gao, B.; Inyang, M.; Zimmerman, A. R.; Cao, X.; Pullammanappallil, P.; Yang, L. Removal of Phosphate from Aqueous Solution by Biochar Derived from Anaerobically Digested Sugar Beet Tailings. *J. Hazard. Mater.* **2011**, *190* (1), 501−507.
(22) Gerente, C.; Lee, V.; Cloirec, P. L.; McKay, G. Application of Chitosan for the Removal of Metals from Wastewaters by Adsorption—Mechanisms and Models Review. *Crit. Rev. Environ. Sci. Technol.* **2007**, *37* (1), 41−127.
(23) Jia, Y.; Steele, C.; Hayward, I.; Thomas, K. Mechanism of Adsorption of Gold and Silver Species on Activated Carbons. *Carbon* **1998**, *36* (9), 1299−1308.
(24) Çelik, Z.; Gülfen, M.; Aydın, A. O. Synthesis of a Novel Dithiooxamide−Formaldehyde Resin and Its Application to the Adsorption and Separation of Silver Ions. *J. Hazard. Mater.* **2010**, *174* (1), 556−562.
(25) Praus, P.; Turicová, M.; Valásková, M. Study of Silver Adsorption on Montmorillonite. *J. Braz. Chem. Soc.* **2008**, *19* (3), 549−556.
(26) Zhang, S.; Peng, F.; Wang, H.; Yu, H.; Zhang, S.; Yang, J.; Zhao, H. Electrodeposition Preparation of Ag Loaded N-Doped TiO_2 Nanotube Arrays with Enhanced Visible Light Photocatalytic Performance. *Catal. Commun.* **2011**, *12* (8), 689−693.
(27) Patterson, A. The Scherrer Formula for X-Ray Particle Size Determination. *Phys. Rev.* **1939**, *56* (10), 978.
(28) Holzwarth, U.; Gibson, N. The Scherrer Equation Versus The 'Debye−Scherrer Equation'. *Nat. Nanotechnol.* **2011**, *6* (9), 534−534.
(29) Huang, Z.; Mills, G.; Hajek, B. Spontaneous Formation of Silver Particles in Basic 2-Propanol. *J. Phys. Chem.* **1993**, *97* (44), 11542−11550.
(30) Kappler, A.; Wuestner, M. L.; Ruecker, A.; Harter, J.; Halama, M.; Behrens, S. Biochar as an Electron Shuttle between Bacteria and Fe(III) Minerals. *Environ. Sci. Technol. Lett.* **2014**, *1* (8), 339−344.
(31) Dong, X.; Ma, L. Q.; Gress, J.; Harris, W.; Li, Y. Enhanced Cr(VI) Reduction and as (III) Oxidation in Ice Phase: Important Role of Dissolved Organic Matter from Biochar. *J. Hazard. Mater.* **2014**, *267*, 62−70.
(32) Dong, X.; Ma, L. Q.; Li, Y. Characteristics and Mechanisms of Hexavalent Chromium Removal by Biochar from Sugar Beet Tailing. *J. Hazard. Mater.* **2011**, *190* (1), 909−915.
(33) Klüpfel, L.; Keiluweit, M.; Kleber, M.; Sander, M. Redox Properties of Plant Biomass-Derived Black Carbon (Biochar). *Environ. Sci. Technol.* **2014**, *48* (10), 5601−5611.
(34) Song, Y.; Shan, D.; Chen, R.; Zhang, F.; Han, E.-H. Formation Mechanism of Phosphate Conversion Film on Mg−8.8 Li Alloy. *Corros. Sci.* **2009**, *51* (1), 62−69.
(35) Yao, Y.; Gao, B.; Zhang, M.; Inyang, M.; Zimmerman, A. R. Effect of Biochar Amendment on Sorption and Leaching of Nitrate, Ammonium, and Phosphate in a Sandy Soil. *Chemosphere* **2012**, *89* (11), 1467−71.
(36) Kowalenko, C.; Yu, S. Assessment of Nitrate Adsorption in Soils by Extraction, Equilibration and Column-Leaching Methods. *Can. J. Soil Sci.* **1996**, *76* (1), 49−57.
(37) Lehmann, J.; Joseph, S. *Biochar for Environmental Management: Science and Technology*; Routledge: London, 2009.
(38) Lu, J.; Cheng, L.; Lau, K. C.; Tyo, E.; Luo, X.; Wen, J.; Miller, D.; Assary, R. S.; Wang, H.-H.; Redfern, P. Effect of the Size-Selective Silver Clusters on Lithium Peroxide Morphology in Lithium−Oxygen Batteries. *Nat. Commun.* **2014**, *5*, 4895.
(39) Yao, Y.; Gao, B.; Fang, J.; Zhang, M.; Chen, H.; Zhou, Y.; Creamer, A. E.; Sun, Y.; Yang, L. Characterization and Environmental Applications of Clay−Biochar Composites. *Chem. Eng. J.* **2014**, *242*, 136−143.

DOI: 10.1021/acsami.5b03131
ACS Appl. Mater. Interfaces 2015, 7, 10634−10640